PLoS one

CSF T-Tau/Aβ$_{42}$ Predicts White Matter Microstructure in Healthy Adults at Risk for Alzheimer's Disease

Barbara B. Bendlin[1,2]*, Cynthia M. Carlsson[1,2], Sterling C. Johnson[1,2], Henrik Zetterberg[3], Kaj Blennow[3], Auriel A. Willette[1,2], Ozioma C. Okonkwo[1,2], Aparna Sodhi[1,2], Michele L. Ries[1,2], Alex C. Birdsill[1,2], Andrew L. Alexander[4,5,6], Howard A. Rowley[7], Luigi Puglielli[1,2], Sanjay Asthana[1,2], Mark A. Sager[1,2]

1 Geriatric Research, Education and Clinical Center (GRECC), William S. Middleton Memorial Veteran's Hospital, Madison, Wisconsin, United States of America, 2 Wisconsin Alzheimer's Disease Research Center, Department of Medicine, University of Wisconsin, Madison, Wisconsin, United States of America, 3 Institute of Neuroscience and Physiology, Department of Psychiatry and Neurochemistry, The Sahlgrenska Academy at University of Gothenburg, Sweden, 4 University of Wisconsin School of Medicine and Public Health, Department of Medical Physics, Madison, Wisconsin, United States of America, 5 University of Wisconsin School of Medicine and Public Health, Department of Psychiatry, Madison, Wisconsin, United States of America, 6 Waisman Laboratory for Brain Imaging and Behavior, Madison, Wisconsin, United States of America, 7 University of Wisconsin School of Medicine and Public Health, Department of Radiology, Madison, Wisconsin, United States of America

Abstract

Cerebrospinal fluid (CSF) biomarkers T-Tau and Aβ$_{42}$ are linked with Alzheimer's disease (AD), yet little is known about the relationship between CSF biomarkers and structural brain alteration in healthy adults. In this study we examined the extent to which AD biomarkers measured in CSF predict brain microstructure indexed by diffusion tensor imaging (DTI) and volume indexed by T1-weighted imaging. Forty-three middle-aged adults with parental family history of AD received baseline lumbar puncture and MRI approximately 3.5 years later. Voxel-wise image analysis methods were used to test whether baseline CSF Aβ$_{42}$, total tau (T-Tau), phosphorylated tau (P-Tau) and neurofilament light protein predicted brain microstructure as indexed by DTI and gray matter volume indexed by T1-weighted imaging. T-Tau and T-Tau/Aβ$_{42}$ were widely correlated with indices of brain microstructure (mean, axial, and radial diffusivity), notably in white matter regions adjacent to gray matter structures affected in the earliest stages of AD. None of the CSF biomarkers were related to gray matter volume. Elevated P-Tau and P-Tau/Aβ$_{42}$ levels were associated with lower recognition performance on the Rey Auditory Verbal Learning Test. Overall, the results suggest that CSF biomarkers are related to brain microstructure in healthy adults with elevated risk of developing AD. Furthermore, the results clearly suggest that early pathological changes in AD can be detected with DTI and occur not only in cortex, but also in white matter.

Introduction

Distinguishing pathologically aging elders from those who will age normally is a key challenge in preventing Alzheimer's disease (AD). Several cerebrospinal fluid (CSF) markers that are presumably related to the core pathology in AD show promise for early detection of the disease. Lower levels of CSF Aβ$_{42}$, higher CSF total tau (T-Tau), and higher tau phosphorylated at threonine 181 (P-Tau$_{181}$), as well as biomarker ratios (T-Tau/Aβ$_{42}$ or P-Tau/Aβ$_{42}$) distinguish patients from controls [1,2,3,4,5] and predict conversion from mild cognitive impairment (MCI) to AD [1,2,6,7,8,9]. When evaluated in cognitively healthy individuals, these biomarkers also appear to be related to cognitive function

[10,11], and measures of brain health that include cortical thinning [12], ventricular expansion and atrophy [11,13,14,15,16].

While studies resulting from volumetric imaging have been very useful for revealing gross structural changes, it is possible that some of the earliest brain changes involved in AD are subtle and below the detection threshold for volumetric imaging. Sensitive to water molecule motion, maps derived from diffusion tensor imaging (DTI) [17] provide unique information on brain microstructure. Mean diffusivity (MD) provides an index of isotropic diffusion of water molecules, and fractional anisotropy (FA) provides a measure of the degree of diffusion anisotropy, both

of which may be altered by tissue damage. Maps based on the principal diffusivities that compose the diffusion tensor may provide additional information on microstructural alterations. The principal diffusivity ($\lambda 1$), or axial diffusivity, represents water diffusion that is parallel to axons and may be altered by axonal injury; radial diffusivity (an average of $\lambda 2$ and $\lambda 3$), represents water diffusion that is perpendicular to axonal fibers and is thus linked to the microstructure of myelin [18,19,20,21,22,23,24,25,26]. DTI has been used to measure disease-related changes in patients with AD [27,28,29,30,31,32,33,34,35,36,37,38,39], as well as alterations in people with MCI [37,40,41,42,43,44,45,46]. Using DTI, microstructural differences have also been detected in presumed presymptomatic AD including participants with APOE4 genotype [47,48,49] family history of AD [50,51], or a combination of both risk factors [52].

In the present study, we examined the relationship between brain microstructure indexed by DTI and proteins associated with brain health in CSF collected in healthy middle-aged and older adults from the Wisconsin Registry for Alzheimer's Prevention [53]. Additionally, because T1-weighted imaging may inform upon atrophy, we assessed the extent to which biomarkers in CSF were related to volume as assessed via T1-weighted imaging. Based on their utility in distinguishing AD patients from controls [1,2,3,4,5], the CSF biomarkers considered in this study were T-Tau, P-Tau$_{181}$, and Aβ_{42}. In addition to these markers of AD pathology, we analyzed CSF for a structural protein of neurons that is predominantly localized in large-caliber axons (and thus likely sensitive to axonal degeneration in white matter): neurofilament light chain protein (NFL) [54]. We hypothesized that baseline CSF measures of these markers would be related to brain health as measured with DTI, especially in brain regions that are affected early in the AD process–principally temporal and cingulate gray and white matter. We expected higher T-Tau and P-Tau and lower Aβ_{42} in CSF would be related to lower FA, higher MD, and altered radial and axial diffusivity in AD-sensitive brain regions. Additionally, we expected that NFL, being sensitive to axonal alteration, would be especially related to axial diffusivity–reflecting altered axonal health. Although the brain regions affected in AD are well known, the relationship between CSF biomarkers and brain health is a relatively new area of study, accordingly we used voxel-wise analyses (corrected for multiple comparisons) [55] to assess relationships across the entire brain.

Materials and Methods

Study procedures were approved by the University of Wisconsin Health Sciences Institutional Review Board and were in accordance with U.S. federal regulations. All participants provided written informed consent.

Participants

We enrolled 47 participants, four of whom were excluded due to unexpected abnormalities found on their MRI scan by the reviewing radiologist (HAR). The remaining 43 middle- to older-aged participants were 37 years of age to 66 years of age at time of lumbar puncture and CSF collection (mean = 53.67, SD = 7.77); and 42 to 71 years of age at time of follow-up scan (mean = 57.61, SD = 8.03). There were 12 men and 31 women. As a group, participants were well educated (mean = 16.26 years, SD = 2.60). All participants were from the Wisconsin Registry for Alzheimer's Prevention (WRAP) [53] and had at least one parent with AD. WRAP is a registry of cognitively normal adults who are followed longitudinally and comprise individuals who have at least one

parent with late onset AD and a group of controls with no family history of AD [53]. To verify the diagnosis of AD in parents of WRAP participants, parental medical records (and autopsy reports where available) were reviewed by a multidisciplinary diagnostic consensus panel. A diagnosis of AD in parents was made using standard clinical criteria [56,57]. There were no families included with known autosomal dominant mutations. In the final sample, three participants had parents who were diagnosed with AD at autopsy, while the remaining clinical diagnoses were confirmed during a consensus meeting. Twelve participants (28%) were carriers of the ε4 allele of the apolipoprotein E (APOE4) gene. Inclusion criteria for all subjects consisted of the following: prior visit for lumbar puncture, normal cognitive function determined by neuropsychological evaluation, no contraindications for MRI and a subsequent normal MRI scan, no current diagnosis of major psychiatric disease or other major medical conditions (e.g., diabetes, myocardial infarction, or recent history of cancer), and no history of head trauma.

Neuropsychological Testing

As part of their participation in WRAP, participants received at least one comprehensive neuropsychological assessment. Neuropsychological testing occurred an average of 1.80 years (SD = 1.28 years) out from the MR scan and 2.06 years (SD = 1.20 years) out from their lumbar puncture. In order to screen for changes in cognitive status, participants who were >3 months out from a neuropsychological testing visit also received the Mini Mental State Examination (MMSE) [58] upon the day of scan. We prospectively identified a subset of tests to examine memory, executive function, and speed of processing. These tests were *BVMT (Brief Visuospatial Memory Test, Revised)* total raw score, and delayed recall, which index visuospatial learning and memory [59]; *COWAT* (Controlled Oral Word Association Test; [60]) seconds to complete/raw score, to assess verbal fluency; *Trail Making Test A & B*, to assess motor speed, sequencing, and vigilance and in Trails B, the additional functions of rapid set shifting, serial retention and integration, verbal problem solving, and planning [61]; Wechsler Adult Intelligence Scale Working Memory Index–a composite of arithmetic, digit span, and letter number sequencing [62]–to assess the ability to hold information in working memory; *RAVLT (Rey Auditory Verbal Learning test)* total over the five learning trials, recognition, and 20 minute delayed recall raw scores [63] to assess immediate and delayed verbal memory.

CSF Collection

The CSF collection was performed via lumbar puncture at a baseline visit in a simvastatin trial [64] an average of 3.41 years prior to brain imaging (SD = 1.19 yrs). CSF samples were collected in the morning after a 12-hour overnight fast, aliquoted in sterile polypropylene collection tubes, and stored in a −80°C freezer. The samples were subsequently sent in one batch to the Sahlgrenska University Hospital at the University of Gothenburg in Sweden for analysis. CSF T-Tau, P-Tau$_{181}$, and Aβ_{42} analysis was accomplished via xMAP technology and utilizing the INNO-BIA AkzBio3 kit (Innogenetics) as previously described [65]. The xMAP technology is based on flow cytometric separation of antibody-coated microspheres that are labeled with a specific mixture of two fluorescent dyes. xMAP allows for simultaneous measurement of several analytes in the same tube, has low intra- and inter-assay variability, and high reproducibility even at low concentrations. NFL was analyzed using the sandwich ELISA method described in [66] with a limit of quantification of 125 ng/L. All analyses were performed on one occasion by certified

laboratory technicians. Intra-assay coefficients of variation were below 10% for all analytes.

Magnetic Resonance Imaging

Participants were invited for brain imaging on the condition that baseline CSF samples were available for analysis. Participants were imaged on a General Electric 3.0 Tesla Discovery MR750 (Waukesha, WI) MRI system with an 8-channel head coil and parallel imaging (ASSET). DTI was acquired using a diffusion-weighted, spin-echo, single-shot, echo planar imaging pulse sequence in 40 encoding directions, B0 = 1300, with eight non-diffusion weighted reference images. The cerebrum was covered using contiguous 2.5 mm thick axial slices, FOV = 24 cm, TR = 8000, E = 67.8, matrix = 96×96, resulting in isotropic 2.5 mm voxels. High order shimming was performed prior to the DTI acquisition to optimize the homogeneity of the magnetic field across the brain and to minimize EPI distortions. A T1-weighted volume was acquired in the axial plane with a 3D fast spoiled gradient-echo (3D EFGRE) sequence using the following parameters: TI = 450 ms; TR = 8.1 ms; TE = 3.2 ms; flip angle = 12°; acquisition matrix = 256×256×156, FOV = 260 mm; slice thickness = 1.0 mm.

MRI Processing

Diffusion-weighted DICOM images were converted into NIFTI format using AFNI (http://afni.nimh.nih.gov/). FA, MD, and lambda maps ($\lambda1$, $\lambda2$ & $\lambda3$) were generated via the FMRIB Software Library (FSL) (http://www.fmrib.ox.ac.uk/fsl/fdt/index.html using the following procedures: (1) image distortions in the DTI data caused by eddy currents were corrected; (2) estimation of diffusion tensors was achieved using DTIFIT; (3) three-dimensional maps of FA, MD, and the 3 eigenvalues ($\lambda1$, $\lambda2$ & $\lambda3$) were computed from the tensors from step (2). Each participant's FA map was aligned to an FA template in Montreal Neurological Institute (MNI) space, comprised of an average of 121 FA maps acquired from healthy participants with similar demographics as the study cohort. Transformations were achieved via 12-parameter affine transformation and nonlinear deformation using Statistical Parametric Mapping software (SPM8 available at http://www.fil.ion.ucl.ac.uk/spm). Estimated transforms from each participant's FA map warping were applied to the participant's remaining DTI maps (MD, $\lambda1$, $\lambda2$ & $\lambda3$) resulting in a transformation of all the original images into MNI space. The normalized FA maps were used to visually inspect for accurate normalization using the "check registration" function in SPM and selecting specific fiber tracts for comparison (corpus callosum, cingulum, superior longitudinal fasciculus). $\lambda2$ & $\lambda3$ maps were averaged to create radial diffusivity maps, and $\lambda1$ was the axial diffusivity map.

Processing of the T1-weighted images was performed using a six class segmentation tool in SPM8. Processing involved bias correction and iterative normalization and segmentation of the original anatomic images [67] into distinct tissue classes (gray matter, white matter, cerebrospinal fluid, skull, fat tissue, and image background) using spatial prior information. Gray matter tissue segments were normalized to MNI template space via a 12-parameter affine transformation and nonlinear deformation (with a warp frequency cutoff of 25). The segmented and normalized gray matter maps were "modulated", which involves scaling the final gray matter maps by the amount of contraction or expansion required to warp the images to the template. The final result was a gray matter probability map for each participant in which the total amount of gray matter remained the same as in the original images. The spatially normalized gray matter maps were

smoothed using an 8-mm Gaussian kernel before being entered into the statistical analysis.

Statistical Analysis

In order to test the relationship between CSF proteins, age, and cognitive function, we performed linear correlation analysis using SPSS (Release 19.0.0, Chicago, SPSS Inc.). CSF biomarkers were log transformed to normalize distribution prior to inclusion in analysis. Differences in CSF protein levels based on APOE status and gender were tested using independent t-tests in SPSS. In order to test the extent to which CSF biomarkers were associated with brain health as indexed by the DTI maps and T1-weighted imaging, voxel-wise linear regression models were implemented via statistical modules available in SPM8. The independent variables were $A\beta_{42}$, total tau (T-Tau), phosphorylated tau (P-Tau$_{181}$), T-Tau/$A\beta_{42}$, and P-Tau$_{181}$/$A\beta_{42}$, while the dependent variables consisted of participants' DTI maps and gray matter probability maps. Due to relatively low levels of NFL in the majority of participants (NFL<125 ng/L; N = 33), NFL was treated as a categorical variable. The detection limit of the assay is NFL<125 ng/L, thus we used this as a cut-point to determine the groups. Differences in brain health based on NFL was tested using voxel-wise ANCOVA, where DTI maps or gray matter probability maps were the dependent variable and the groups were NFL>125 ng/L, and NFL<125 ng/L. Age (at time of MR scan) and gender were included as covariates in all models due to known effects on brain microstructure [68,69,70,71]. Because the imaging was performed in a group of participants that had been randomized in a simvastatin trial, only baseline (pre-simvastatin) CSF measures were used and a treatment vs. placebo covariate was included in the statistical models. All analyses were thresholded at p<.05 corrected for multiple comparisons using false discovery rate (FDR) correction [72]. In order to exclude small clusters and increase the anatomical plausibility of the results, a cluster size threshold of 50 contiguous voxels was used and analyses were restricted to gray and white matter using a binary brain mask. The binary brain mask was computed by thresholding the SPM brain mask in MNI space (which contains voxels that vary from 0 percent to 100 percent probability of brain) at a threshold of.5 or greater (50% probability or greater of being brain). Furthermore, analysis of the gray matter probability maps used an absolute threshold masking of 0.1 to exclude voxels with a low probability of being gray matter.

Results

Demographics, Neuropsychological Function, and CSF Biomarkers

There was a significant positive correlation (P<.05) between age at time of lumbar puncture and T-Tau, T-Tau/$A\beta_{42}$, and P-Tau$_{181}$/$A\beta_{42}$ (Pearson correlation coefficients for age and CSF markers are shown in **Table 1**). Men and women did not differ on CSF biomarker levels of T-Tau, P-Tau$_{181}$, $A\beta_{42}$, T-Tau/$A\beta_{42}$, or P-Tau$_{181}$/$A\beta_{42}$. There was a significant difference in T-Tau and $A\beta_{42}$ between APOE4 positive and APOE4 negative participants, where T-Tau was higher in the non-carriers (m = 4.25) compared to carriers (m = 3.90), t(41) = 2.038, p<.05, and $A\beta_{42}$ was lower in the carriers (m = 5.57) compared to non-carriers (m = 5.83), t(41) = 3.062, p<.05. APOE4 carriers and non-carriers did not differ on age (p = .78).

All participants were cognitively normal as determined by comprehensive neuropsychological testing and as assessed by MMSE (MMSE ≥27). Controlling for age and education, linear correlation analysis indicated that baseline CSF biomarker levels

Table 1. Linear correlation among CSF biomarkers and age.

		Age	T-Tau	P-Tau$_{181}$	Aβ$_{42}$	T-Tau/Aβ$_{42}$
Age	Pearson Correlation					
T-Tau	Pearson Correlation	0.367 *				
P-Tau$_{181}$	Pearson Correlation	0.253	0.585 Ŧ			
Aβ$_{42}$	Pearson Correlation	−0.147	0.256	0.228		
T-Tau/Aβ$_{42}$	Pearson Correlation	0.443 *	0.856 Ŧ	0.459 *	−0.281	
P-Tau$_{181}$/Aβ$_{42}$	Pearson Correlation	0.326 *	0.436 *	0.854 Ŧ	−0.310 *	0.599 Ŧ

Significant correlation at P<.05 *.
Significant at p<.001 Ŧ.
doi:10.1371/journal.pone.0037720.t001

were related to a subset of the neuropsychological test scores. WAIS Working Memory Index (scaled for age and education) was positively correlated with T-Tau (r = .307, p<.05) and with T-Tau/Aβ$_{42}$ (r = 0.303, p = .051). However, a scatter-plot revealed that the participant with the highest tau value (>2 SD higher than the mean) performed well on working memory–skewing the results. When this participant was removed from the analysis, the relationships were no longer significant. RAVLT recognition score was negatively correlated with both P-Tau$_{181}$ (r = −.379, p<.05) and P-Tau$_{181}$/Aβ$_{42}$ (r = −.362, p<.05) but was not related to T-Tau, Aβ$_{42}$, or their ratio. No other RAVLT sub-scores or other neuropsychological tests were significantly correlated with the CSF markers.

Imaging Results

Voxel-wise regression analysis indicated that both T-Tau and T-Tau/Aβ$_{42}$ showed robust and widespread positive relationships with several of the DTI measures, specifically MD, axial and radial diffusion. These relationships were extensive in white matter and were prevalent in temporal, parietal and frontal lobes. The locations of peak T-value for MD and FA clusters obtained in the voxel-wise analysis are tabulated in **Table 2** (axial and radial diffusivity results are tabulated in **Table S1**). The brain regions where CSF T-Tau/Aβ$_{42}$ predicted MD values in the voxel-wise regression analysis are shown in **Figure 1**; the positive relationship between T-Tau/Aβ$_{42}$ and MD is shown in **Figure 2** in scatter plots from a subset of the significant clusters found in the voxel-wise regression analysis. The regional overlap between T-Tau and T-Tau/Aβ$_{42}$ SPM result maps (MD, axial and radial diffusivity) was extensive, and is summarized in terms of percent overlap in **Table 3**.

At a statistical threshold of p<.05 (FDR corrected for multiple comparisons) there was no relationship between T-Tau or T-Tau/Aβ$_{42}$ and FA. Furthermore, neither P-Tau$_{181}$ nor P-Tau/Aβ$_{42}$ were related to any of the DTI measures (FA, MD, axial or radial diffusivity). Higher Aβ$_{42}$ in CSF was related to higher FA in medial frontal gyrus, but not related to MD, axial or radial diffusivity. Participants with NFL>125 ng/L showed a single region of higher FA in middle temporal gyrus white matter compared to control, with no differences in MD, axial or radial diffusivity. Complete results (cluster extent, T-value, and locations) for all CSF measures and FA and MD maps are in **Table 2** (axial and radial diffusivity results are tabulated in **Table S1**). None of the CSF biomarkers predicted gray matter volume as indexed by the modulated gray matter probability maps (FDR p<.05).

Discussion

General

AD-related CSF biomarkers are linked with global and regional brain volumes in healthy elderly [12,13,14]. In this study, we assessed the relationship between brain tissue microstructure measured with DTI and AD-related CSF biomarkers. Additionally, we assessed the relationship between CSF biomarkers and gray matter volume. Our group has previously found that cognitively healthy people with parental family history of AD show microstructural brain differences compared to those without risk for AD [50]. In this study, we found that CSF biomarkers previously associated with AD are related to brain tissue microstructure in similar regions as those previously found to be associated with parental family history.

While gray matter volume was not related to any of the CSF biomarkers in this study, CSF biomarkers were related to white matter health as indexed by DTI; interestingly, the regions of significant association were mostly *adjacent* to critical gray matter structures that are known to be affected in AD. This was especially true for T-Tau and T-Tau/Aβ$_{42}$, where higher CSF levels were related to higher axial, radial, and mean diffusivity in a large swath of temporal lobe white matter adjacent to hippocampus. Several studies now point toward early involvement of white matter in AD development, including human studies on AD risk [48,49,50,52,73], and studies on a triple transgenic mouse model of AD indicating white matter changes may precede other measurable pathology in AD [74,75]. In contrast, studies conducted in AD and memory impaired patients have found that CSF biomarker levels are related to gray matter structures including hippocampus, entorhinal cortex [76], and posterior cingulate cortex [77], One possibility is that early AD pathology involves axonal or myelin degeneration and that cortical change is only measurable at later disease stages or in more elderly individuals.

White Matter Degeneration in AD: Myelin and Axons

White matter degeneration in diagnosed AD is confirmed by several human post mortem studies [78,79,80,81]. MRI enabled ante mortem studies substantiate post mortem findings, showing decreased regional white matter volumes in AD compared to controls [82,83,84,85,86,87,88,89,90,91,92] and differences in water diffusion properties in white matter [27,28,29,30,31,32,33,34,35,36,37,93]. White matter alterations in confirmed AD are a combination of axonal and myelin alteration, yet it is unknown whether white matter changes are secondary to damage of the neuronal soma, involve primary axonal
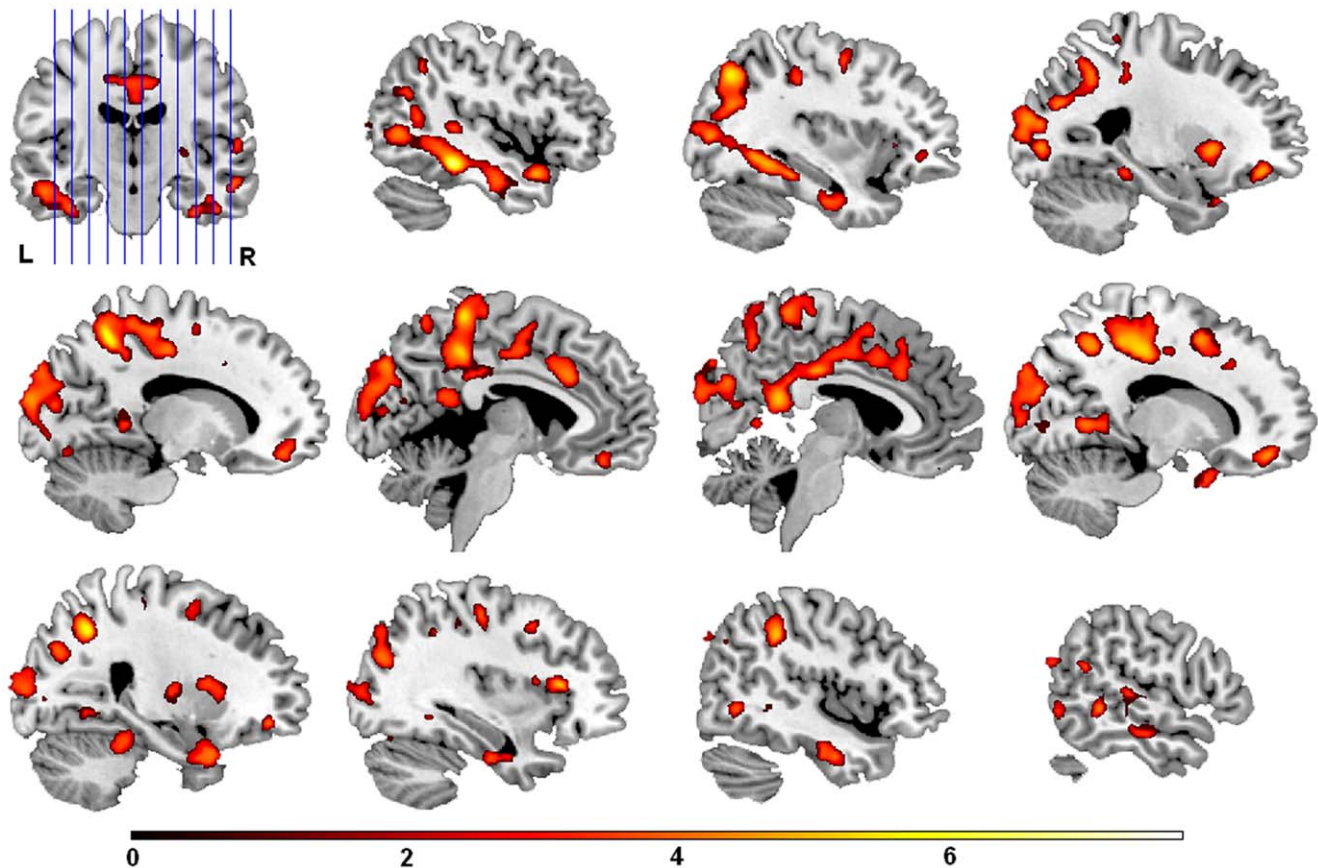
Figure 1. CSF T-Tau/Aβ42 and mean diffusivity. Higher T-Tau/Aβ42 at baseline was associated with increased mean diffusivity in follow-up scanning in several brain regions, encompassing both gray and white matter. As shown above, this relationship was especially prominent in temporal lobe white matter adjacent to hippocampus, but also encompassing gray and white matter in frontal and parietal lobes, portions of occipital white matter, and small clusters in cerebellum. Results are FDR corrected for multiple comparisons (p<.05) and displayed here with a cluster size threshold of 20 or more voxels. Sections are shown in sagittal view beginning from the left side of the brain to right. Variations in the color map reflect the size of the T-statistic (indexed by the color bar at bottom).
doi:10.1371/journal.pone.0037720.g001

degeneration [94,95], are linked with myelin degeneration [39,46,96,97,98], or represent some combination of these events.

In our study we measured the relationship between CSF biomarkers and DTI measures that are presumably related to axonal health (axial diffusivity) and myelin health (radial diffusivity). We found that both T-Tau and T-Tau/Aβ$_{42}$ predicted axial and radial diffusivity, suggesting these CSF biomarkers are potentially related to both neuronal axon integrity and health of oligodendrocyte synthesized myelin. Furthermore, the analyses of axial, radial, and mean diffusivity produced statistical maps that were highly overlapping, suggesting that alterations in one cell component (e.g. neuronal axons) could very well be associated with related alterations in another cell component (myelin).

Although CSF measures of myelin were not available to us in this study, we assessed axonal degeneration via CSF measured neurofilament light protein. Neurofilament proteins are major constituents of the axonal cytoskeleton, consisting of three polypeptides; light (NFL), medium and heavy subunits. NFL proteins are most related to large-caliber axons [99] and when axons are damaged, NFL is released into CSF. NFL proteins measured in CSF are significantly higher in AD compared to controls [66,100,101,102,103,104]. In our study,a group comparison based on CSF NFL levels yielded a single region of difference in middle temporal gyrus white matter, where participants with

higher CSF NFL showed higher FA. Although we expected that the group with presumably greater axonal degeneration would show lower FA, it's possible that early stage axonal degeneration in the presence of intact myelin could lead to higher anisotropy. Another possibility is a loss of crossing fibers in this region–which could lead to higher FA. Although we did not find a relationship between CSF NFL and the mean, radial, and axial diffusivity maps at a relatively conservative statistical threshold, analyses performed at uncorrected (for multiple comparisons) thresholds did show differences between NFL groups. Interestingly, the group with higher CSF NFL showed higher axial diffusivity in cingulum and white matter adjacent to hippocampus. Because only ten participants in our study had NFL levels greater than the detection limit of 125 ng/L, we were likely underpowered to find these subtle differences at corrected thresholds and further work will be needed to expand upon these preliminary findings.

Classic Pathology: Abnormal Phosphorylation of Tau and Amyloid Deposition

In AD, abnormal phosphorylation of tau protein and deposition of amyloid are considered primary processes underlying neuronal degeneration. Hyperphosphorylation of tau and its subsequent release from the cell means markers of tau measured in CSF increase compared to controls [105]. In contrast, CSF markers of
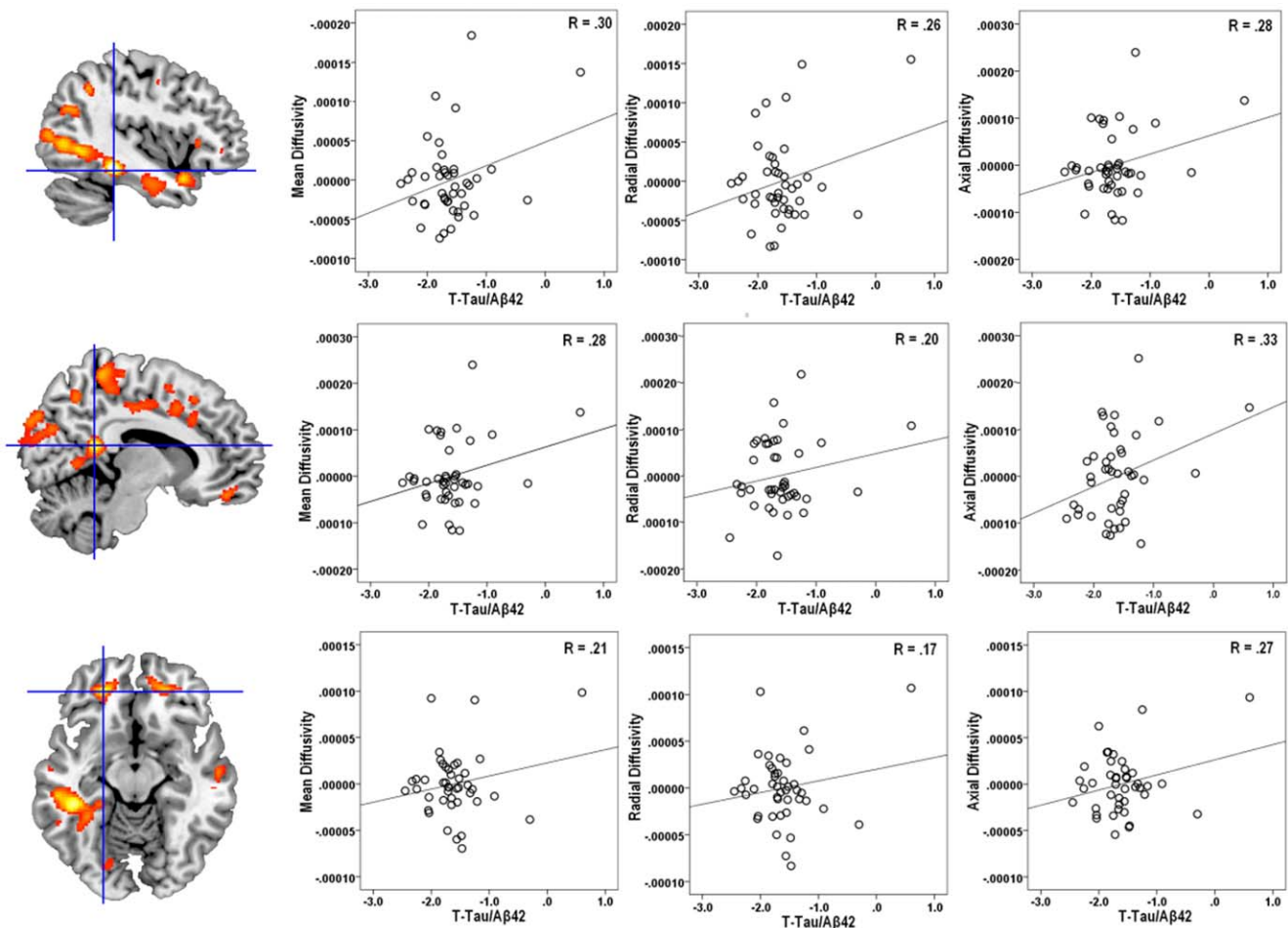
Figure 2. T-Tau/Aβ42 Plotted against mean, radial, and axial diffusivity. Shown here are the results of the voxel-wise analysis, where regions with color overlay are those where higher T-Tau/Aβ42 was associated with higher diffusivity (mean, radial, and axial). In order to illustrate the relationship between T-Tau/Aβ42 and the diffusivity maps, we extracted diffusion values from representative regions of significant correlation in the voxel-wise analysis and plotted them against T-Tau/Aβ42. Shown on the top row are diffusion values extracted from the left temporal lobe ($x = -42$, $y = -34$, $z = -16$) plotted against T-Tau/Aβ42. In the middle row are diffusion values extracted from right posterior cingulum bundle ($x = 8$, $y = -46$, $z = 16$) plotted against T-Tau/Aβ42. In the bottom row are diffusion values extracted from left inferior frontal white matter ($x = -22$, $y = 43$, $z = -12$) plotted against T-Tau/Aβ42. Blue crosshairs overlaid on the brain sections indicate the location of the extracted values. Each point in the scatter represents diffusion values from one participant ($n = 43$). T-Tau/Aβ42 values were log-transformed and mean, radial, and axial diffusivity values were adjusted for age at time of scan, sex, and treatment (CSF data were collected at baseline in a Simvastatin treatment trial, data from the prevention trial are not shown here).
doi:10.1371/journal.pone.0037720.g002

amyloid decrease as amyloid is deposited in the brain [3,4,106,107]. In our study, we found widespread relationships between elevated CSF T-Tau and altered measures of brain tissue microstructure indexed by mean, radial, and axial diffusivity, with somewhat similar but also distinctive patterns occurring for T-Tau/Aβ42 (up to 70% overlap in the radial diffusivity maps). Although the localized source of tau protein measured in CSF is unknown, higher levels in our study were related to higher diffusion across temporal, parietal, and frontal lobes–particularly in white matter. We speculate CSF tau protein may have originated from axons in these brain regions, but we can not rule out that tau may have also originated from oligodendroglia [108]. Phosphorylation of tau is associated with the development of glial tangles in human patients with AD [109,110,111], as well as in animals expressing mutant tau [112,113,114]. Interestingly, CSF levels of tau phosphorylated at threonine 181 did not show a relationship with any of the DTI measures at the $p < .05_{FDR}$ threshold. Although some studies suggest that CSF P-Tau$_{181}$ does

not correlate with neuropathological burden in AD [115], in our study it is possible that the relationship between P-Tau$_{181}$ and tissue microstructure was too subtle to survive our statistical threshold. Indeed, when we performed exploratory analyses at uncorrected (for multiple comparisons) thresholds, higher P-Tau$_{181}$ was associated with altered tissue microstructure. Furthermore, P-Tau$_{181}$ and P-Tau$_{181}$/Aβ42 were the only biomarkers related to memory function in this study. Nonetheless, considering alternative sites of tau phosphorylation will likely be important for understanding early AD and in AD biomarker development.

While T-Tau and T-Tau/Aβ42 showed widespread relationships with the DTI measures, CSF Aβ42 was associated with lower anisotropy of water (FA) only in medial frontal cortex and underlying white matter. Deposition of brain amyloid in AD likely involves frontal involvement at the earliest stages [116], which presumably could have resulted in altered tissue microstructure in this study. Studies using amyloid imaging in this cohort are

Table 2. Regions where CSF biomarkers were significantly correlated with FA and MD in the voxel-wise analyses.

	MNI coordinates x y z	Peak T value	k (mm³)
T-Tau & Fractional Anisotropy	×	×	×
T-Tau & Mean Diffusivity			
R Parietal Lobe WM	26, −59, 42	7.89	13890
R Medial Frontal Gyrus	16, 7, 52	6.37	478
L Middle Frontal Gyrus	−24, 43, −14	5.83	259
R Middle Temporal Gyrus	58, −42, −1	5.33	159
L Frontal Lobe, WM	−18, −4, 59	5.25	154
R Corpus Callosum	12, −45, 12	5.23	414
R Medial Frontal WM	12, 46, −18	5.21	207
L Superior Temporal Gyrus WM	−60, −23, 7	4.73	112
R Lentiform Nucleus, Putamen	26, −9, 7	4.45	256
R Superior Temporal Gyrus WM	60, −24, −1	4.39	145
L Temporal Lobe WM	−52, −13, −21	4.37	143
L Inferior Frontal Gyrus	−40, 25, 3	4.25	56
R Fusiform WM	38, −71, −21	4.06	83
R Entorhinal WM	20, 11, −28	3.99	110
R Lingual Gyrus	28, −61, −4	3.96	74
R Middle Temporal Gyrus	46, −63, −6	3.91	52
L Inferior Parietal Lobule	−52, −41, 40	3.75	63
P-Tau & Fractional Anisotropy	×	×	×
P-Tau & Mean Diffusivity	×	×	×
Aβ₄₂ & Fractional Anisotropy			
L,R Medial Frontal Gyrus	0 11 −24	6.27	66
Aβ₄₂ & Mean Diffusivity	×	×	×
T-Tau/Aβ₄₂ & Fractional Anisotropy	×	×	×
T-Tau/Aβ₄₂ & Mean Diffusivity			
L Temporal Lobe WM	−44 −36 −13	7.71	11374
R Uncus	20 9 −27	6.11	286
L Middle Frontal Gyrus WM	−22 43 −12	5.69	257
R Insula WM	36 26 11	5.50	229
R Supramarginal Gyrus WM	44 −39 39	5.17	225
R Medial Frontal Gyrus WM	12 46 −16	5.09	204
R Middle Temporal Gyrus	58 −42 −1	5.07	126
L Superior Temporal Gyrus	−42 13 −22	5.05	157
L Putamen	−24 14 0	5.01	100
R Middle Temporal Gyrus	48 −63 −4	4.87	105
R Superior Temporal Gyrus WM	58 −24 5	4.68	154
L Superior Temporal Gyrus WM	−62 −21 7	4.54	109
R Temporal Lobe WM	42 −6 −31	4.48	209
L Superior Temporal Gyrus WM	−62 −43 14	4.41	99
R Superior Occipital Gyrus WM	34 −77 26	4.23	409
R Occipital Lobe WM	28 −59 −4	4.20	87
R Middle Temporal Gyrus WM	56 −14 −16	4.04	76
R Precentral Gyrus WM	34 −22 51	3.91	100
L Frontal Lobe WM	−30 −35 39	3.82	100
R Cerebellum, Anterior Lobe	24 −37 −21	3.78	118
R Putamen	28 −10 3	3.76	82
P-Tau/Aβ₄₂ & Fractional Anisotropy	×	×	×
P-Tau/Aβ₄₂ & Mean Diffusivity	×	×	×

Table 2. Cont.

	MNI coordinates x y z	Peak T value	k (mm^3)
NFL & Fractional Anisotropy			
L Middle Temporal Gyrus WM	−42 −65 11	6.66	40
NFL & Mean Diffusivity	–	–	–

MNI: Montreal Neurological Institute; k: cluster size; T-Tau: Total Tau; P-Tau: Phosphorylated Tau; WM: White Matter; L: Left; R: Right.
× No relationship with any regions at FDR corrected threshold p<.05.
− No group differences in any region at FDR corrected threshold p<.05.
doi:10.1371/journal.pone.0037720.t002

expected to shed further light on regional amyloid deposition in the earliest stages of AD.

CSF Biomarkers in Cognitively Healthy Adults

In healthy older adults, levels of AD biomarkers measured in CSF are related to age, cognition, structural brain volume, and AD risk factors including APOE4 status [10,117,118] and family history [51]. In our sample of healthy adults with elevated risk for AD, we found significant positive correlations between age and T-Tau, T-Tau/Aβ_{42}, and P-Tau$_{181}$/Aβ_{42}. Alone, Aβ_{42} was not related to age. We also found that both T-Tau and Aβ_{42} differed between APOE4 carriers and non-carriers. Similar to previous studies, Aβ_{42} was lower in the carriers compared to non-carriers–conceivably suggesting greater amyloid deposition in the group at greater risk for AD. Interesting, we found that the APOE4 carriers in this sample showed lower T-Tau compared to non-carriers. These T-Tau findings are consistent with our previous report on CSF biomarkers in middle-aged at-risk adults [119]. Although APOE4 has been linked with higher T-Tau in some studies [120,121], our sample differs in that all of the participants were positive for parental family history of AD–a group which in middle age shows higher T-Tau levels than the general population [51]. Further studies will be needed to dissociate the effects of APOE and family history of AD on CSF biomarkers in middle-age.

All of the participants in our study tested cognitively normal. Among the cognitive tests, only recognition memory was related to any of the CSF measures. Participants with higher P-Tau$_{181}$ and P-Tau$_{181}$/Aβ_{42} levels had lower recognition on a list learning test (RAVLT). Glodzik et al. have also found a relationship between P-Tau (P-Tau$_{231}$) and memory function [11], and combined use of P-Tau$_{181}$ and Aβ_{42} has also been shown to predict longitudinal subjective memory impairment in healthy elderly [122]. Because our study was cross-sectional and restricted to cognitively healthy participants, the limited range and variability of the cognitive

scores may have impacted our power to detect relationships between the CSF biomarkers and other cognitive tests in our study.

Previous brain imaging studies in healthy adults have found that CSF biomarkers are related to volumetric measures. Healthy elderly individuals from ADNI with low CSF Aβ_{42} levels have significantly higher whole brain loss over time, ventricular expansion, and greater rates of hippocampal atrophy [14]. Fjell et al. [13] also examined CSF biomarker and brain relationships in healthy elderly individuals from ADNI. Lower Aβ_{42} correlated with 1-year change in several regions including putamen, thalamus, superior temporal cortex, cingulate, and frontal brain regions, whereas higher T-Tau/Aβ_{42} was related to atrophy in amygdala, paracentral cortex, and ventricular regions. Higher P-Tau was related to 1-year change in amygdala, paracentral cortex, posterior cingulate, and pallidum. Fjell et al.'s study is also one of the few to show a relationship between P-Tau and cerebral white matter, with higher P-Tau predicting lower white matter volume. P-Tau reported in these studies was assayed for tau phosphorylated at threonine 181, although a similarly aged healthy cohort evaluated at baseline and 2 years later by Glodzik et al. [11] has shown that P-Tau$_{231}$ is also associated with longitudinal medial temporal lobe volume decline and memory function.

In our study of adults with parental family history of AD and a high frequency of APOE4, we found relationships between CSF measures and DTI in several brain regions shown in previous volumetric studies of healthy participants, including temporal, cingulate, and frontal cortices. We did not find a relationship between the CSF biomarkers and gray matter volume (indexed by T1-weighted imaging) in any brain regions, possibly due to the younger age of our cohort in whom tissue changes are likely to be more subtle and less easily detected with volumetric imaging. Using DTI, we had the additional advantage of being able to

Table 3. Percent of regional overlap between statistical parametric mapping result maps.

	T-Tau & MD	T-Tau & Rad.	T-Tau & Ax.	T-Tau/Aβ_{42} & Ax.	T-Tau/Aβ_{42} & Rad.
T-Tau/Aβ_{42} & MD*	66%	74%	60%	85%	95%
T-Tau/Aβ_{42} & Rad. Diff.	57%	70%	49%	68%	
T-Tau/Aβ_{42} & Ax. Diff.	54%	58%	58%		
T-Tau & Ax. Diff.	84%	83%			
T-Tau & Rad. Diff.	70%				

All results maps were the product of a linear correlation analysis, where the CSF measures (T-Tau and T-Tau/Aβ42) were used to predict the diffusion measures (MD, axial and radial diffusivity). T-Tau: Total Tau; MD: Mean Diffusivity; Rad: Radial; Ax: Axial; Diff: Diffusivity.
*Result map shown in Figure 1.
doi:10.1371/journal.pone.0037720.t003

evaluate potentially subtle effects in white matter, and these relationships were robust and widespread.

Limitations

While the results of this study are promising, potential limitations should be noted. We adopted a voxel-wise approach in order to assess the extent to which CSF biomarkers were related to brain microstructure and volume across gray and white matter tissue. While we took great care to evaluate for potential errors during registration of the DTI maps to a common template, methods that employ registration to a template may be susceptible to subtle error and statistical effects may be influenced by the size of smoothing filters used in voxel-wise analyses. As a further comment on the DTI results, we would like to note that this study used a tensor model which resolves a single fiber direction within each voxel. We found very robust results when analyzing the MD, axial, and radial diffusivity maps, compared to the FA maps. Due to the complex architecture of white matter, employing FA derived from the tensor model may not have captured the full information available with alternative methods of DTI acquisition and higher order modeling [123]. We should also note that our population was composed solely of participants with parental family history of AD and the frequency of APOE4 was 28%. While this group is at increased risk for AD and thus provides a powerful cohort for examining AD biomarkers, the lack of family history negative participants and high frequency of APOE4 potentially limits the generalizability of our results to a healthy population in addition to limiting our ability to measure relationships between CSF biomarkers and brain measures that are independent of AD risk. Additionally, although our study was longitudinal in the sense that baseline CSF was collected followed by MRI acquisition approximately three and a half years later, simultaneous MRI and CSF collection over two or more time points would have yielded greater power to map out longitudinal change in these measures. Based on the results of this study, additional longitudinal work is warranted. Finally, while our results begin to address the pattern of white matter changes that may occur in the earliest stages of AD, employing white matter biomarker assays in larger cohorts of older adults is expected to clarify the nature of white matter changes in the earliest disease stages.

Summary

CSF biomarkers previously associated with AD are related to brain tissue microstructure. This study supports an emerging theory that brain white matter alterations are an early event in AD pathogenesis. The mechanisms that underlie white matter alterations and the nature of these alterations deserve further study.

Supporting Information

Table S1 Regions where CSF biomarkers were significantly correlated with axial and radial diffusivity in the voxel-wise analyses.
(DOC)

Acknowledgments

Author Contributions

Conceived and designed the experiments: BBB CMC LP. Performed the experiments: BBB CMC HZ KB AAW MLR ALA HAR SA MAS. Analyzed the data: BBB CMC HZ KB AAW ACB MLR AS ALA SCJ. Contributed reagents/materials/analysis tools: HZ KB ALA. Wrote the paper: BBB CMC SCJ HZ KB AAW OCO AS MLR ACB ALA HAR LP SA MAS.

References

1. De Meyer G, Shapiro F, Vanderstichele H, Vanmechelen E, Engelborghs S, et al. (2010) Diagnosis-independent Alzheimer disease biomarker signature in cognitively normal elderly people. Arch Neurol 67: 949–956.

2. Shaw LM, Vanderstichele H, Knapik-Czajka M, Clark CM, Aisen PS, et al. (2009) Cerebrospinal fluid biomarker signature in Alzheimer's disease neuroimaging initiative subjects. Ann Neurol 65: 403–413.

3. Galasko D, Chang L, Motter R, Clark CM, Kaye J, et al. (1998) High cerebrospinal fluid tau and low amyloid beta42 levels in the clinical diagnosis of Alzheimer disease and relation to apolipoprotein E genotype. Arch Neurol 55: 937–945.

4. Sunderland T, Linker G, Mirza N, Putnam KT, Friedman DL, et al. (2003) Decreased beta-amyloid1–42 and increased tau levels in cerebrospinal fluid of patients with Alzheimer disease. Jama 289: 2094–2103.

5. Smach MA, Charfeddine B, Ben Othman L, Lammouchi T, Dridi H, et al. (2009) Evaluation of cerebrospinal fluid tau/beta-amyloid(42) ratio as diagnostic markers for Alzheimer disease. Eur Neurol 62: 349–355.

6. Davatzikos C, Bhatt P, Shaw LM, Batmanghelich KN, Trojanowski JQ (2011) Prediction of MCI to AD conversion, via MRI, CSF biomarkers, and pattern classification. Neurobiol Aging.

7. Hampel H, Teipel SJ, Fuchsberger T, Andreasen N, Wiltfang J, et al. (2004) Value of CSF beta-amyloid1–42 and tau as predictors of Alzheimer's disease in patients with mild cognitive impairment. Mol Psychiatry 9: 705–710.

8. Hansson O, Zetterberg H, Buchhave P, Andreasson U, Londos E, et al. (2007) Prediction of Alzheimer's disease using the CSF Abeta42/Abeta40 ratio in patients with mild cognitive impairment. Dement Geriatr Cogn Disord 23: 316–320.

9. Mattsson N, Zetterberg H, Hansson O, Andreasen N, Parnetti L, et al. (2009) CSF biomarkers and incipient Alzheimer disease in patients with mild cognitive impairment. Jama 302: 385–393.

10. Fagan AM, Roe CM, Xiong C, Mintun MA, Morris JC, et al. (2007) Cerebrospinal fluid tau/beta-amyloid(42) ratio as a prediction of cognitive decline in nondemented older adults. Arch Neurol 64: 343–349.

11. Glodzik L, de Santi S, Tsui WH, Mosconi L, Zinkowski R, et al. (2011) Phosphorylated tau 231, memory decline and medial temporal atrophy in normal elders. Neurobiol Aging.

12. Desikan RS, Sabuncu MR, Schmansky NJ, Reuter M, Cabral HJ, et al. (2010) Selective disruption of the cerebral neocortex in Alzheimer's disease. PLoS One 5: e12853.

13. Fjell AM, Walhovd KB, Fennema-Notestine C, McEvoy LK, Hagler DJ, et al. (2010) Brain atrophy in healthy aging is related to CSF levels of Abeta1–42. Cereb Cortex 20: 2069–2079.

14. Schott JM, Bartlett JW, Fox NC, Barnes J (2010) Increased brain atrophy rates in cognitively normal older adults with low cerebrospinal fluid Abeta1–42. Ann Neurol 68: 825–834.

15. Ott BR, Cohen RA, Gongvatana A, Okonkwo OC, Johanson CE, et al. (2010) Brain ventricular volume and cerebrospinal fluid biomarkers of Alzheimer's disease. J Alzheimers Dis 20: 647–657.

16. Fagan AM, Head D, Shah AR, Marcus D, Mintun M, et al. (2009) Decreased cerebrospinal fluid Abeta(42) correlates with brain atrophy in cognitively normal elderly. Ann Neurol 65: 176–183.

17. Basser PJ, Pierpaoli C (1996) Microstructural and physiological features of tissues elucidated by quantitative-diffusion-tensor MRI. J Magn Reson B 111: 209–219.

18. Hofling AA, Kim JH, Fantz CR, Sands MS, Song SK (2009) Diffusion tensor imaging detects axonal injury and demyelination in the spinal cord and cranial nerves of a murine model of globoid cell leukodystrophy. NMR Biomed.

19. Feng S, Hong Y, Zhou Z, Xiaofeng D, et al. (2009) Monitoring of acute axonal injury in the swine spinal cord with EAE by diffusion tensor imaging. J Magn Reson Imaging 30: 277–285.

20. Mac Donald CL, Dikranian K, Bayly P, Holtzman D, Brody D (2007) Diffusion tensor imaging reliably detects experimental traumatic axonal injury and indicates approximate time of injury. J Neurosci 27: 11869–11876.

21. Sun SW, Liang HF, Trinkaus K, Cross AH, Armstrong RC, et al. (2006) Noninvasive detection of cuprizone induced axonal damage and demyelination in the mouse corpus callosum. Magn Reson Med 55: 302–308.

22. Song SK, Yoshino J, Le TQ, Lin SJ, Sun SW, et al. (2005) Demyelination increases radial diffusivity in corpus callosum of mouse brain. Neuroimage 26: 132–140.

23. Song SK, Sun SW, Ramsbottom MJ, Chang C, Russell J, et al. (2002) Dysmyelination revealed through MRI as increased radial (but unchanged axial) diffusion of water. Neuroimage 17: 1429–1436.

24. Harsan LA, Poulet P, Guignard B, Steibel J, Parizel N, et al. (2006) Brain dysmyelination and recovery assessment by noninvasive in vivo diffusion tensor magnetic resonance imaging. J Neurosci Res 83: 392–402.

25. Budde MD, Kim JH, Liang HF, Russell JH, Cross AH, et al. (2007) Axonal injury detected by in vivo diffusion tensor imaging correlates with neurological disability in a mouse model of multiple sclerosis. NMR Biomed.

26. Wu Q, Butzkueven H, Gresle M, Kirchhoff F, Friedhuber A, et al. (2007) MR diffusion changes correlate with ultra-structurally defined axonal degeneration in murine optic nerve. Neuroimage 37: 1138–1147.

27. Bozzali M, Falini A, Franceschi M, Cercignani M, Zuffi M, et al. (2002) White matter damage in Alzheimer's disease assessed in vivo using diffusion tensor magnetic resonance imaging. J Neurol Neurosurg Psychiatry 72: 742–746.

28. Fellgiebel A, Schermuly I, Gerhard A, Keller I, Albrecht J, et al. (2008) Functional relevant loss of long association fibre tracts integrity in early Alzheimer's disease. Neuropsychologia 46: 1698–1706.

29. Hanyu H, Asano T, Sakurai H, Imon Y, Iwamoto T, et al. (1999) Diffusion-weighted and magnetization transfer imaging of the corpus callosum in Alzheimer's disease. J Neurol Sci 167: 37–44.

30. Huang J, Friedland RP, Auchus AP (2007) Diffusion tensor imaging of normal-appearing white matter in mild cognitive impairment and early Alzheimer disease: preliminary evidence of axonal degeneration in the temporal lobe. AJNR Am J Neuroradiol 28: 1943–1948.

31. Rose SE, Janke AL, Chalk JB (2008) Gray and white matter changes in Alzheimer's disease: a diffusion tensor imaging study. J Magn Reson Imaging 27: 20–26.

32. Salat DH, Tuch DS, van der Kouwe AJ, Greve DN, Pappu V, et al. (2008) White matter pathology isolates the hippocampal formation in Alzheimer's disease. Neurobiol Aging.

33. Stahl R, Dietrich O, Teipel SJ, Hampel H, Reiser MF, et al. (2007) White matter damage in Alzheimer disease and mild cognitive impairment: assessment with diffusion-tensor MR imaging and parallel imaging techniques. Radiology 243: 483–492.

34. Takahashi S, Yonezawa H, Takahashi J, Kudo M, Inoue T, et al. (2002) Selective reduction of diffusion anisotropy in white matter of Alzheimer disease brains measured by 3.0 Tesla magnetic resonance imaging. Neurosci Lett 332: 45–48.

35. Xie S, Xiao JX, Gong GL, Zang YF, Wang YH, et al. (2006) Voxel-based detection of white matter abnormalities in mild Alzheimer disease. Neurology 66: 1845–1849.

36. Duan JH, Wang HQ, Xu J, Lin X, Chen SQ, et al. (2006) White matter damage of patients with Alzheimer's disease correlated with the decreased cognitive function. Surg Radiol Anat 28: 150–156.

37. Medina D, deToledo-Morrell L, Urresta F, Gabrieli JDE, Moseley M, et al. (2006) White matter changes in mild cognitive impairment and AD: A diffusion tensor imaging study. Neurobiology of Aging 27: 663–672.

38. Canu E, McLaren DG, Fitzgerald ME, Bendlin BB, Zoccatelli G, et al. (2009) Microstructural Diffusion Changes are Independent of Macrostructural Volume Loss in Moderate to Severe Alzheimer's Disease. J Alzheimers Dis.

39. Stricker NH, Schweinsburg BC, Delano-Wood L, Wierenga CE, Bangen KJ, et al. (2009) Decreased white matter integrity in late-myelinating fiber pathways in Alzheimer's disease supports retrogenesis. Neuroimage 45: 10–16.

40. Cho H, Yang DW, Shon YM, Kim BS, Kim YI, et al. (2008) Abnormal integrity of corticocortical tracts in mild cognitive impairment: a diffusion tensor imaging study. J Korean Med Sci 23: 477–483.

41. Fellgiebel A, Wille P, Muller MJ, Winterer G, Scheurich A, et al. (2004) Ultrastructural hippocampal and white matter alterations in mild cognitive impairment: a diffusion tensor imaging study. Dement Geriatr Cogn Disord 18: 101–108.

42. Kantarci K, Jack CR, Jr., Xu YC, Campeau NG, O'Brien PC, et al. (2001) Mild cognitive impairment and Alzheimer disease: regional diffusivity of water. Radiology 219: 101–107.

43. Lovblad KO, Delavelle J, Wetzel S, Kelekis AD, Assal F, et al. (2004) ADC mapping of the aging frontal lobes in mild cognitive impairment. Neuroradiology 46: 282–286.

44. Rose SE, McMahon KL, Janke AL, O'Dowd B, de Zubicaray G, et al. (2006) Diffusion indices on magnetic resonance imaging and neuropsychological performance in amnestic mild cognitive impairment. J Neurol Neurosurg Psychiatry 77: 1122–1128.

45. Fellgiebel A, Muller MJ, Wille P, Dellani PR, Scheurich A, et al. (2005) Color-coded diffusion-tensor-imaging of posterior cingulate fiber tracts in mild cognitive impairment. Neurobiol Aging 26: 1193–1198.

46. Stenset V, Bjornerud A, Fjell AM, Walhovd KB, Hofoss D, et al. (2009) Cingulum fiber diffusivity and CSF T-tau in patients with subjective and mild cognitive impairment. Neurobiol Aging.

47. Nierenberg J, Pomara N, Hoptman MJ, Sidtis JJ, Ardekani BA, et al. (2005) Abnormal white matter integrity in healthy apolipoprotein E epsilon4 carriers. Neuroreport 16: 1369–1372.

48. Persson J, Lind J, Larsson A, Ingvar M, Cruts M, et al. (2006) Altered brain white matter integrity in healthy carriers of the APOE epsilon4 allele: a risk for AD? Neurology 66: 1029–1033.

49. Ryan L, Walther K, Bendlin BB, Lue LF, Walker DG, et al. (2011) Age-related differences in white matter integrity and cognitive function are related to APOE status. Neuroimage 54: 1565–1577.

50. Bendlin BB, Ries ML, Canu E, Sodhi A, Lazar M, et al. (2010) White matter is altered with parental family history of Alzheimer's disease. Alzheimers Dement 6: 394–403.

51. Xiong C, Roe CM, Buckles V, Fagan A, Holtzman D, et al. (2011) Role of Family History for Alzheimer Biomarker Abnormalities in the Adult Children Study. Arch Neurol 68: 1313–1319.

52. Smith CD, Chebrolu H, Andersen AH, Powell DA, Lovell MA, et al. (2010) White matter diffusion alterations in normal women at risk of Alzheimer's disease. Neurobiol Aging 31: 1122–1131.

53. Sager MA, Hermann B, La Rue A (2005) Middle-aged children of persons with Alzheimer's disease: APOE genotypes and cognitive function in the Wisconsin Registry for Alzheimer's Prevention. J Geriatr Psychiatry Neurol 18: 245–249.

54. Olsson B, Zetterberg H, Hampel H, Blennow K (2011) Biomarker-based dissection of neurodegenerative diseases. Prog Neurobiol.

55. Ashburner J, Friston KJ (2000) Voxel-based morphometry–the methods. Neuroimage 11: 805–821.

56. Morris JC, Heyman A, Mohs RC, Hughes JP, van Belle G, et al. (1989) The Consortium to Establish a Registry for Alzheimer's Disease (CERAD). Part I. Clinical and neuropsychological assessment of Alzheimer's disease. Neurology 39: 1159–1165.

57. McKhann G, Drachman D, Folstein M, Katzman R, Price D, et al. (1984) Clinical diagnosis of Alzheimer's disease: Report of the NINCDS-ADRDA workgroup under the auspices of the Department of Health and Human Services Task Force on Alzheimer's disease. Neurology 34: 939–944.

58. Folstein MF, Folstein SE, McHugh PR (1975) "Mini Mental State": a practical method for grading the cognitive state of patients for the clinician. Journal of Psychiatry Research 12: 189–198.

59. Benedict R (1997) Brief Visuospatial Memory Test-Revised. Lutz, FL: Psychological Assessment Resources Inc.

60. Benton AL, Hamsher K, Sivan AB (1983) Multilingual Aphasia Examination. Iowa City: AJA Associates.

61. Reitan RM, Wolfson D (1993) The Halstead-Reitan Neuropsychological Test Battery: Theory and clinical interpretation. Tucson: Neuropsychology Press.

62. Wechsler D (1997) Wechsler Adult Intelligence Scale-Third Edition. New York: Psych Corp.

63. Rey A (1964) L'examen clinique en psychologie. Paris: Presses Universitaires de France.

64. Carlsson CM, Gleason CE, Johnson SC, Xu G, Huang Y, et al. (2010) A randomized, double-blind placebo-controlled trial of simvastatin on CSF, MRI, and cognitive biomarkers in middle-aged adults at risk for Alzheimer's disease: The ESPRIT Study. Alzheimer's and Dementia 6: S151–S152.

65. Olsson A, Vanderstichele H, Andreasen N, De Meyer G, Wallin A, et al. (2005) Simultaneous measurement of beta-amyloid(1–42), total tau, and phosphorylated tau (Thr181) in cerebrospinal fluid by the xMAP technology. Clin Chem 51: 336–345.

66. Rosengren LE, Karlsson JE, Karlsson JO, Persson LI, Wikkelso C (1996) Patients with amyotrophic lateral sclerosis and other neurodegenerative diseases have increased levels of neurofilament protein in CSF. J Neurochem 67: 2013–2018.

67. Ashburner J, Friston KJ (2005) Unified segmentation. Neuroimage 26: 839–851.

68. Bendlin BB, Fitzgerald ME, Ries ML, Xu G, Kastman EK, et al. (2010) White matter in aging and cognition: a cross-sectional study of microstructure in adults aged eighteen to eighty-three. Dev Neuropsychol 35: 257–277.

69. Pfefferbaum A, Sullivan EV, Hedehus M, Lim KO, Adalsteinsson E, et al. (2000) Age-related decline in brain white matter anisotropy measured with spatially corrected echo-planar diffusion tensor imaging. Magn Reson Med 44: 259–268.

70. Salat DH, Tuch DS, Greve DN, van der Kouwe AJ, Hevelone ND, et al. (2005) Age-related alterations in white matter microstructure measured by diffusion tensor imaging. Neurobiol Aging 26: 1215–1227.

71. Menzler K, Belke M, Wehrmann E, Krakow K, Lengler U, et al. (2011) Men and women are different: diffusion tensor imaging reveals sexual dimorphism in the microstructure of the thalamus, corpus callosum and cingulum. Neuroimage 54: 2557–2562.

72. Genovese CR, Lazar NA, Nichols T (2002) Thresholding of statistical maps in functional neuroimaging using the false discovery rate. Neuroimage 15: 870–878.

73. Bartzokis G, Lu PH, Geschwind DH, Tingus K, Huang D, et al. (2007) Apolipoprotein E affects both myelin breakdown and cognition: implications for age-related trajectories of decline into dementia. Biol Psychiatry 62: 1380–1387.

74. Desai MK, Guercio BJ, Narrow WC, Bowers WJ (2011) An Alzheimer's disease-relevant presenilin-1 mutation augments amyloid-beta-induced oligodendrocyte dysfunction. Glia 59: 627–640.

75. Desai MK, Sudol KL, Janelsins MC, Mastrangelo MA, Frazer ME, et al. (2009) Triple-transgenic Alzheimer's disease mice exhibit region-specific

abnormalities in brain myelination patterns prior to appearance of amyloid and tau pathology. Glia 57: 54–65.

76. Herukka SK, Pennanen C, Soininen H, Pirttila T (2008) CSF Abeta42, tau and phosphorylated tau correlate with medial temporal lobe atrophy. J Alzheimers Dis 14: 51–57.

77. Sole-Padulles C, Llado A, Bartres-Faz D, Fortea J, Sanchez-Valle R, et al. (2011) Association between cerebrospinal fluid tau and brain atrophy is not related to clinical severity in the Alzheimer's disease continuum. Psychiatry Res 192: 140–146.

78. de la Monte SM (1989) Quantitation of cerebral atrophy in preclinical and end-stage Alzheimer's disease. Ann Neurol 25: 450–459.

79. Scheltens P, Barkhof F, Leys D, Wolters EC, Ravid R, et al. (1995) Histopathologic correlates of white matter changes on MRI in Alzheimer's disease and normal aging. Neurology 45: 883–888.

80. Bronge L, Bogdanovic N, Wahlund LO (2002) Postmortem MRI and histopathology of white matter changes in Alzheimer brains. A quantitative, comparative study. Dement Geriatr Cogn Disord 13: 205–212.

81. Roher AE, Weiss N, Kokjohn TA, Kuo YM, Kalback W, et al. (2002) Increased A beta peptides and reduced cholesterol and myelin proteins characterize white matter degeneration in Alzheimer's disease. Biochemistry 41: 11080–11090.

82. Li S, Pu F, Shi F, Xie S, Wang Y, et al. (2008) Regional white matter decreases in Alzheimer's disease using optimized voxel-based morphometry. Acta Radiol 49: 84–90.

83. Stout JC, Jernigan TL, Archibald SL, Salmon DP (1996) Association of dementia severity with cortical gray matter and abnormal white matter volumes in dementia of the Alzheimer type. Arch Neurol 53: 742–749.

84. Salat DH, Greve DN, Pacheco JL, Quinn BT, Helmer KG, et al. (2009) Regional white matter volume differences in nondemented aging and Alzheimer's disease. Neuroimage 44: 1247–1258.

85. Im K, Lee JM, Won Seo S, Hyung Kim S, Kim SI, et al. (2008) Sulcal morphology changes and their relationship with cortical thickness and gyral white matter volume in mild cognitive impairment and Alzheimer's disease. Neuroimage 43: 103–113.

86. Balthazar ML, Yasuda CL, Pereira FR, Pedro T, Damasceno BP, et al. (2009) Differences in grey and white matter atrophy in amnestic mild cognitive impairment and Alzheimer's disease. Eur J Neurol 16: 468–474.

87. Chaim TM, Duran FL, Uchida RR, Perico CA, de Castro CC, et al. (2007) Volumetric reduction of the corpus callosum in Alzheimer's disease in vivo as assessed with voxel-based morphometry. Psychiatry Res 154: 59–68.

88. Baxter LC, Sparks DL, Johnson SC, Lenoski B, Lopez JE, et al. (2006) Relationship of cognitive measures and gray and white matter in Alzheimer's disease. J Alzheimers Dis 9: 253–260.

89. Teipel SJ, Hampel H, Alexander GE, Schapiro MB, Horwitz B, et al. (1998) Dissociation between corpus callosum atrophy and white matter pathology in Alzheimer's disease. Neurology 51: 1381–1385.

90. Teipel SJ, Bayer W, Alexander GE, Zebuhr Y, Teichberg D, et al. (2002) Progression of corpus callosum atrophy in Alzheimer disease. Arch Neurol 59: 243–248.

91. Vermersch P, Scheltens P, Barkhof F, Steinling M, Leys D (1994) Evidence for atrophy of the corpus callosum in Alzheimer's disease. Eur Neurol 34: 83–86.

92. Wang PJ, Saykin AJ, Flashman LA, Wishart HA, Rabin LA, et al. (2006) Regionally specific atrophy of the corpus callosum in AD, MCI and cognitive complaints. Neurobiol Aging 27: 1613–1617.

93. Mielke MM, Kozauer NA, Chan KC, George M, Toroney J, et al. (2009) Regionally-specific diffusion tensor imaging in mild cognitive impairment and Alzheimer's disease. Neuroimage 46: 47–55.

94. Terry RD (1998) The cytoskeleton in Alzheimer disease. J Neural Transm Suppl 53: 141–145.

95. Stokin GB, Lillo C, Falzone TL, Brusch RG, Rockenstein E, et al. (2005) Axonopathy and transport deficits early in the pathogenesis of Alzheimer's disease. Science 307: 1282–1288.

96. Bartzokis G, Sultzer D, Lu PH, Nuechterlein KH, Mintz J, et al. (2004) Heterogeneous age-related breakdown of white matter structural integrity: implications for cortical "disconnection" in aging and Alzheimer's disease. Neurobiol Aging 25: 843–851.

97. Bartzokis G, Lu PH, Tishler TA, Fong SM, Oluwadara B, et al. (2007) Myelin breakdown and iron changes in Huntington's disease: pathogenesis and treatment implications. Neurochem Res 32: 1655–1664.

98. Bartzokis G (2004) Age-related myelin breakdown: a developmental model of cognitive decline and Alzheimer's disease. Neurobiol Aging 25: 5–18; author reply 49–62.

99. Friede RL, Samorajski T (1970) Axon caliber related to neurofilaments and microtubules in sciatic nerve fibers of rats and mice. Anat Rec 167: 379–387.

100. Sjogren M, Blomberg M, Jonsson M, Wahlund LO, Edman A, et al. (2001) Neurofilament protein in cerebrospinal fluid: a marker of white matter changes. J Neurosci Res 66: 510–516.

101. Norgren N, Rosengren L, Stigbrand T (2003) Elevated neurofilament levels in neurological diseases. Brain Res 987: 25–31.

102. Hu YY, He SS, Wang XC, Duan QH, Khatoon S, et al. (2002) Elevated levels of phosphorylated neurofilament proteins in cerebrospinal fluid of Alzheimer disease patients. Neurosci Lett 320: 156–160.

103. Rosengren LE, Karlsson JE, Sjogren M, Blennow K, Wallin A (1999) Neurofilament protein levels in CSF are increased in dementia. Neurology 52: 1090–1093.

104. Andreasen N, Gottfries J, Vanmechelen E, Vanderstichele H, Davidson P, et al. (2001) Evaluation of CSF biomarkers for axonal and neuronal degeneration, gliosis, and beta-amyloid metabolism in Alzheimer's disease. J Neurol Neurosurg Psychiatry 71: 557–558.

105. Vandermeeren M, Mercken M, Vanmechelen E, Six J, van de Voorde A, et al. (1993) Detection of tau proteins in normal and Alzheimer's disease cerebrospinal fluid with a sensitive sandwich enzyme-linked immunosorbent assay. J Neurochem 61: 1828–1834.

106. Fagan AM, Mintun MA, Mach RH, Lee SY, Dence CS, et al. (2006) Inverse relation between in vivo amyloid imaging load and cerebrospinal fluid Abeta42 in humans. Ann Neurol 59: 512–519.

107. Tapiola T, Alafuzoff I, Herukka SK, Parkkinen L, Hartikainen P, et al. (2009) Cerebrospinal fluid {beta}-amyloid 42 and tau proteins as biomarkers of Alzheimer-type pathologic changes in the brain. Arch Neurol 66: 382–389.

108. Richter-Landsberg C (2008) The cytoskeleton in oligodendrocytes. Microtubule dynamics in health and disease. J Mol Neurosci 35: 55–63.

109. Iwatsubo T, Hasegawa M, Ihara Y (1994) Neuronal and glial tau-positive inclusions in diverse neurologic diseases share common phosphorylation characteristics. Acta Neuropathol 88: 129–136.

110. Umahara T, Tsuchiya K, Ikeda K, Kanaya K, Iwamoto T, et al. (2002) Demonstration and distribution of tau-positive glial coiled body-like structures in white matter and white matter threads in early onset Alzheimer's disease. Neuropathology 22: 9–12.

111. Nishimura M, Tomimoto H, Suenaga T, Namba Y, Ikeda K, et al. (1995) Immunocytochemical characterization of glial fibrillary tangles in Alzheimer's disease brain. Am J Pathol 146: 1052–1058.

112. Gotz J, Chen F, Barmettler R, Nitsch RM (2001) Tau filament formation in transgenic mice expressing P301L tau. J Biol Chem 276: 529–534.

113. Higuchi M, Ishihara T, Zhang B, Hong M, Andreadis A, et al. (2002) Transgenic mouse model of tauopathies with glial pathology and nervous system degeneration. Neuron 35: 433–446.

114. Lin WL, Lewis J, Yen SH, Hutton M, Dickson DW (2003) Filamentous tau in oligodendrocytes and astrocytes of transgenic mice expressing the human tau isoform with the P301L mutation. Am J Pathol 162: 213–218.

115. Buerger K, Alafuzoff I, Ewers M, Pirttila T, Zinkowski R, et al. (2007) No correlation between CSF tau protein phosphorylated at threonine 181 with neocortical neurofibrillary pathology in Alzheimer's disease. Brain 130: e82.

116. Braak H, Braak E (1997) Frequency of stages of Alzheimer-related lesions in different age categories. Neurobiol Aging 18: 351–357.

117. Kester MI, Blankenstein MA, Bouwman FH, van Elk EJ, Scheltens P, et al. (2009) CSF biomarkers in Alzheimer's disease and controls: associations with APOE genotype are modified by age. J Alzheimers Dis 16: 601–607.

118. Sunderland T, Mirza N, Putnam KT, Linker G, Bhupali D, et al. (2004) Cerebrospinal fluid beta-amyloid1–42 and tau in control subjects at risk for Alzheimer's disease: the effect of APOE epsilon4 allele. Biol Psychiatry 56: 670–676.

119. Carlsson CM, Gleason CE, Hess TM, Moreland KA, Blazel HM, et al. (2008) Effects of simvastatin on cerebrospinal fluid biomarkers and cognition in middle-aged adults at risk for Alzheimer's disease. J Alzheimers Dis 13: 187–197.

120. Andersson C, Blennow K, Johansson SE, Almkvist O, Engfeldt P, et al. (2007) Differential CSF biomarker levels in APOE-epsilon4-positive and -negative patients with memory impairment. Dement Geriatr Cogn Disord 23: 87–95.

121. Herukka SK, Hallikainen M, Soininen H, Pirttila T (2005) CSF Abeta42 and tau or phosphorylated tau and prediction of progressive mild cognitive impairment. Neurology 64: 1294–1297.

122. Stomrud E, Hansson O, Zetterberg H, Blennow K, Minthon L, et al. (2010) Correlation of longitudinal cerebrospinal fluid biomarkers with cognitive decline in healthy older adults. Arch Neurol 67: 217–223.

123. Tournier JD, Mori S, Leemans A (2011) Diffusion tensor imaging and beyond. Magn Reson Med 65: 1532–1556.